

Interactive comment on “A global finite-element shallow-water model supporting continuous and discontinuous elements” by P. A. Ullrich

P. A. Ullrich

pauullrich@ucdavis.edu

Received and published: 8 October 2014

Author uses some “local” high-order schemes to construct the global shallow water models on cubed-sphere grid in this manuscript. The “local” high-order schemes are suitable for constructing global atmospheric models due to many reasons and getting popular recently. Different schemes under the same framework using FR method are adopted and compared by author through checking the benchmark tests for SWE model on sphere. It is a very interesting study for this community. I recommend the publication of this manuscript subject to the following revisions.

I would like to thank the reviewer for his very helpful comments on this manuscript.

1. *Although the high-order models give many impressive results in the smooth cases,*

C1939

an effective limiter is necessary for any high-order model to correctly simulate the discontinuities even for atmospheric flows. The artificial viscosity was introduced in this study and may improve the results near the discontinuities to some extent. Is there any further plan to develop other better methods to deal with the discontinuities?

There is significant interest in pursuing the problem of limiting finite element calculations for tracer transport (see for instance Guba (2014)), but the interest is far less for dynamics calculations. High resolution calculations with the spectral element dynamical core in CESM (which runs at $n_p = 4$) have shown that topography needs to be greatly smoothed to reduce noise in the vicinity of sharp elevation changes. This effect clearly reflects the issue you have pointed out, although it is not clear what kind of effect monotonization would have on the simulated climate.

Reference: Guba, Oksana, Mark Taylor, and Amik St-Cyr. "Optimization-based limiters for the spectral element method." *Journal of Computational Physics* 267 (2014): 176-195.

2. *I would like to see the numerical results of the Rossby-Haurwitz wave (Williamson's test case 6). To my knowledge, this test is sensitive to the numerical viscosity. Please check this test using different schemes with and without the artificial viscosity.*

Results for the Rossby-Haurwitz wave are given in Fig. 1 and 2 for $n_e = 16$ horizontal resolution. As pointed out, there are significant differences in the height field which are induced by the addition of the hyperviscosity operator (although both results appear reasonable given the coarse horizontal resolution). Some of the previous observations still hold: SE is unstable without the addition of hyperviscosity, whereas DG with penalization is effective at stabilizing the method for both lumped and non-lumped variants. The maximum stable time step size shows a similar pattern to that of the mountain-induced Rossby wave train.

Figure 1 Caption: Height field with $n_e = 16$ and $n_p = 4$ at day 14 for the Rossby-Haurwitz wave with (a) continuous elements and hyperviscosity (reference solution).

C1940

Height difference plot from reference solution with $n_e = 16$ at day 14 for (b) discontinuous g_2 elements with hyperviscosity, (c) discontinuous g_1 elements with hyperviscosity, (d) continuous elements without hyperviscosity, (e) discontinuous g_2 elements without hyperviscosity and (f) discontinuous g_1 elements without hyperviscosity. The time step used for these runs was (a,d) $\Delta t = 480$ s, (b,e) $\Delta t = 200$ s and (c,f) $\Delta t = 120$ s. Discontinuous penalization was used for both discontinuous schemes. Contour spacing is 1 m in plots (b) and (c) and 20 m in plots (d), (e) and (f). Long dashed lines show the cubed-sphere grid.

Figure 2 Caption: Normalized total energy and potential enstrophy change for the Rossby-Haurwitz wave test with $n_e = 16$ and $n_p = 4$ over a 15 day simulation. In (a) and (b) all simulations show roughly equivalent energy and enstrophy loss and so all lines are coincident. In (c) and (d) the simulation with continuous elements is beginning to experience instability, leading to total energy and enstrophy growth after approximately 6 days simulation time.

3. *FR method is a general framework for the arbitrary high-order schemes. Why do you chose $n_p=4$? Have you ever tried the higher order schemes?*

A thorough investigation of different values of n_p would greatly extend the length of the manuscript, so I settled on one value of n_p , chosen in accordance with the current value of n_p for the Community Atmosphere Model spectral element dynamical core and Ullrich (2013). This medium-order choice has the advantage of greatly improving on the treatment of waves over lower-order methods, but does not suffer from the increased computational expense of much higher-order methods.

Reference: Ullrich, P.A. (2013) "Understanding the treatment of waves in atmospheric models, Part I: The shortest resolved waves of the 1D linearized shallow water equations" *Quart. J. Roy. Meteor. Soc.*, Volume 140, Issue 682, pp. 1426–1440, DOI: 10.1002/qj.2226.

4. *Please check the balanced setup of barotropic instability test. In Chen et al., JCP, C1941*

2014, the evolution patterns of l1 errors are different on three different grids (see their Fig.23). On cubed-sphere grid, at the beginning of the simulation the l1 error becomes much larger compared with other two grids and will not decrease on the refined grids. Will you find the similar issues using your models?

I find that in this model setup there is convergence with resolution of all three error norms (at fourth-order), but this convergence does not occur until at least $n_e = 40$. Presumably there are fine-scale features in the barotropic instability test which are not resolved on the grid scale until this resolution is reached. Similar results have been observed in an analogous fourth-order cubed-sphere finite-volume code that is described in an upcoming manuscript in CAMCoS.

Interactive comment on Geosci. Model Dev. Discuss., 7, 5141, 2014.

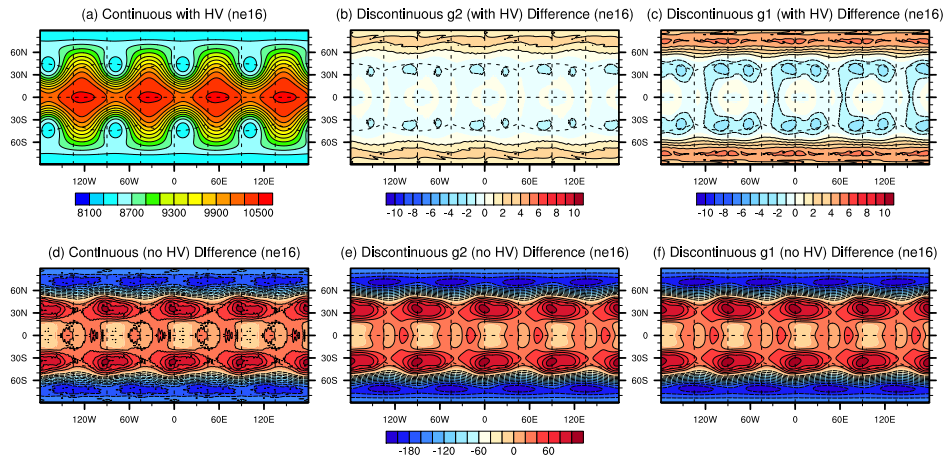


Fig. 1.

C1943

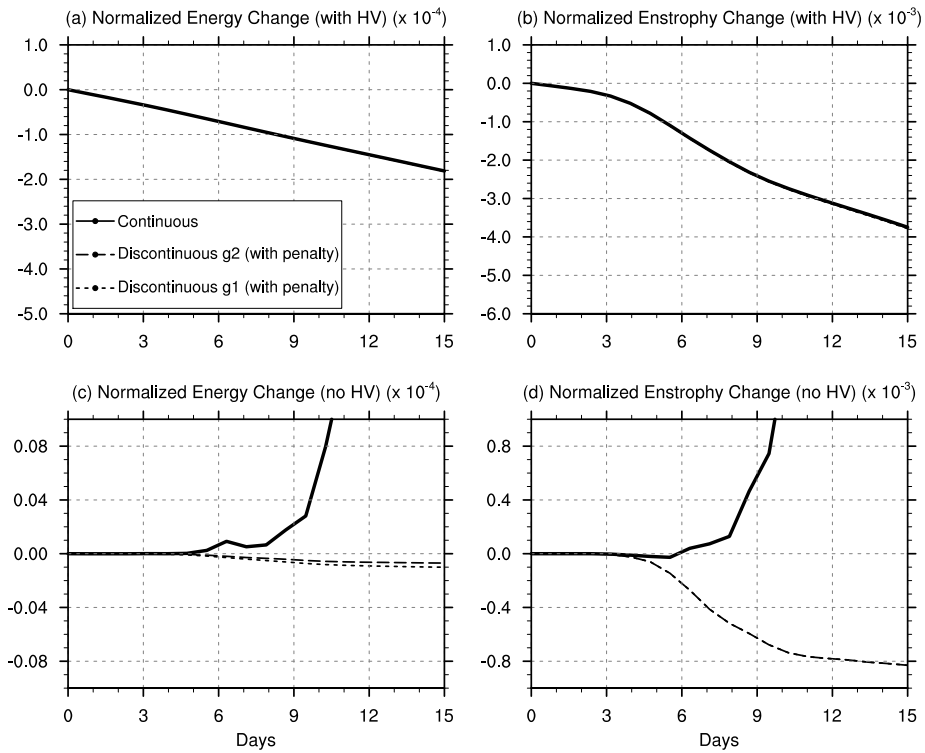


Fig. 2.

C1944